Firing Variability of Frontal Pole Neurons during a Cued Strategy Task

Satoshi Tsujimoto[1,2] and Aldo Genovesio[3]

Abstract

■ In previous reports, we described neuronal activity in the polar (PFp), dorsolateral (PFdl), and orbital (PFo) PFC as monkeys performed a cued strategy task with two spatial goals. On each trial, a cue instructed one of two strategies: Stay with the previous goal or shift to the alternative. A delay period followed each cue, and feedback followed each choice, also at a delay. Our initial analysis showed that the mean firing rate of a population of PFp cells encoded the goal chosen on a trial, but only near the time of feedback, not earlier in the trial. In contrast, PFdl cells encoded goals and strategies during the cue and delay periods, and PFo cells encoded strategies in those task periods. Both areas also signaled goals near feedback time. Here we analyzed trial-to-trial variability of neuronal firing, as measured by the Fano factor (FF): the ratio of variance to the mean. Goal-selective PFp neurons had two properties: (1) a lower FF from the beginning of the trial compared with PFp cells that did not encode goals and (2) a weak but significant inverse correlation between FF throughout a trial and the degree of goal selectivity at feedback time. Cells in PFdl and PFo showed neither of these properties. Our findings indicate that goal-selective PFp neurons were engaged in the task throughout a trial, although they only encoded goals near feedback time. Their lower FF could improve the ability of other cortical areas to decode its selected-goal signal. ■

INTRODUCTION

The polar PFC (PFp) is situated at the rostral extreme of the primate PFC, and it is thought to have evolved either in early primates or during anthropoid evolution (Preuss & Goldman-Rakic, 1991). On the basis of neuroimaging and lesion studies in humans, it has been suggested to play a role in a variety of higher cognitive functions, including relational reasoning, exploratory decisions, prospective memory, higher-level sequential behavior, and evaluative judgments, among others (Koechlin, 2016; Desrochers, Chatham, & Badre, 2015; Bludau et al., 2014; Tsujimoto, Genovesio, & Wise, 2011b; Badre & D'Esposito, 2009; Ramnani, Elliott, Athwal, & Passingham, 2004; Ramnani & Owen, 2004; Christoff, Ream, Geddes, & Gabrieli, 2003). Unfortunately, technical difficulties have impeded a study of its neurophysiology in macaque monkeys until recently (Mitz, Tsujimoto, Maclarty, & Wise, 2009).

To bridge this gap, we recorded single-cell activity from PFp of monkeys while they performed a cued strategy task (Tsujimoto, Genovesio, & Wise, 2010, 2012). The results showed that PFp neurons did not encode any task-related variables until just before and just after the expected feedback (feedback time). This temporally restricted task period occurred after the monkey had been given a strategy cue, chosen a spatial goal, and implemented that choice via a saccadic eye movement. Around feedback time, PFp neurons encoded the spatial goal that the monkey had chosen on that trial: left or right from a central fixation point.

To explore further the properties of PFp neurons, here we studied the trial-to-trial variability of firing rates in the same neuronal population as described in our previous reports. A reduction in firing rate variability is thought to improve the reliability and precision of a neural code (Churchland et al., 2010; Shadlen & Newsome, 1998), and it has been shown to be a sensitive measure of the engagement of neurons in various components of cognitive behavior (Qi & Constantinidis, 2015; Hussar & Pasternak, 2010). Recent studies have suggested that trial-to-trial variability conveys information about a monkey's cognitive or behavioral state, such as the perception of external signals in sensory areas (Churchland et al., 2010), motor preparation in premotor areas (Churchland, Yu, Ryu, Santhanam, & Shenoy, 2006), including in the FEF (Purcell, Heitz, Cohen, & Schall, 2012), attentional states in area V4 (Mitchell, Sundberg, & Reynolds, 2007), and, in PFC, both general task engagement (Hussar & Pasternak, 2010) and the state of operant conditioning (Qi & Constantinidis, 2012). Accordingly, we measured the firing rate variability in PFp and compared it with the same measure in the dorsolateral and orbital PFC (PFdl and PFo, respectively). This analysis took advantage of the finding that neurons in these two PFC areas—unlike PFp—encoded

[1]Kyoto University, [2]Nielsen Consumer Neuroscience, Tokyo, Japan, [3]University of Rome

Journal of Cognitive Neuroscience 29:1, pp. 25–36
doi:10.1162/jocn_a_01036

task-related information during the periods substantially before feedback time, such as the cue and delay periods (Tsujimoto et al., 2012; Tsujimoto, Genovesio, & Wise, 2009, 2011a). The temporally restricted goal encoding of PFp neurons also contrasted with the cognitive demands of the cued strategy task. During the pre-cue period of each trial, this task required the monkeys to maintain their previous spatial goal in short-term (working) memory. During the cue and delay periods, the monkeys needed to identify and implement a behavioral strategy and use that strategy to select a spatial goal for the upcoming saccade. The present analysis explores the neural correlates of both this temporally extensive task engagement and the temporally restricted goal encoding of PFp neurons.

METHODS

Subjects

Two male rhesus monkeys (*Macaca mulatta*), weighing 10–11 kg, were operantly conditioned to perform saccade tasks before recordings began. During task performance, each monkey sat in a primate chair, with its head stabilized and oriented toward a video monitor 32 cm away. Their eye position was recorded by an infrared oculometer (Arrington Research, Inc., Scottsdale, AZ). All procedures conformed to the Guide for the Care and Use of Laboratory Animals and were approved by the appropriate institutional animal care and use committee.

Behavioral Tasks

We used a cued-strategy task (Figure 1A) that has been described previously (Tsujimoto et al., 2010, 2011a, 2012). After an intertrial interval of 1 sec, the fixation point (a 0.6° filled white circle) is presented at the center of the video screen, along with two potential saccade targets (2.0° unfilled white squares) located 11.6° to the left and right of the fixation point. To begin a trial, the monkeys had to attain and maintain fixation on the central point for 1.5 sec. A cue period of 0.5 sec followed this pre-cue fixation period of 1.5 sec. The cue differed by task (Figure 1B) and was either visually cued or fluid-reward cued. In the visually cued strategy task, the cue consisted of a square (2.0° × 2.0°) or rectangle (1.0° × 4.9°) that appeared at the fixation point (Figure 1B). On each trial, one cue was selected pseudorandomly from a set of four: a vertical rectangle (light gray), a horizontal rectangle of the same dimensions and brightness, a yellow square, and a purple square of the same size (Figure 1B). In the fluid-reward cued strategy task, one drop of fluid (0.2 mL) or two half-drops of fluid (0.1 mL each) was delivered as a cue at the beginning of the cue period (Figure 1B) instead of a visual stimulus. The vertical rectangle, yellow square, and one drop of fluid were called "stay cues" and instructed the "stay" strategy; that is, select the same response on the current trial as on the previous trial. The horizontal rectangle, purple square, and two half-drops of fluid were called "shift cues" and instructed the "shift" strategy; that is, shift from the previous response. Given that there were only two potential responses, namely, a saccade to either left or right targets, a shift cue determined the response and reward probability in the same way as a stay cue. In both cases, the most recent correct and rewarded response served as the reference for the current response. A given block of trials in the visually cued task included approximately equal numbers of four visual cues and two possible responses. In

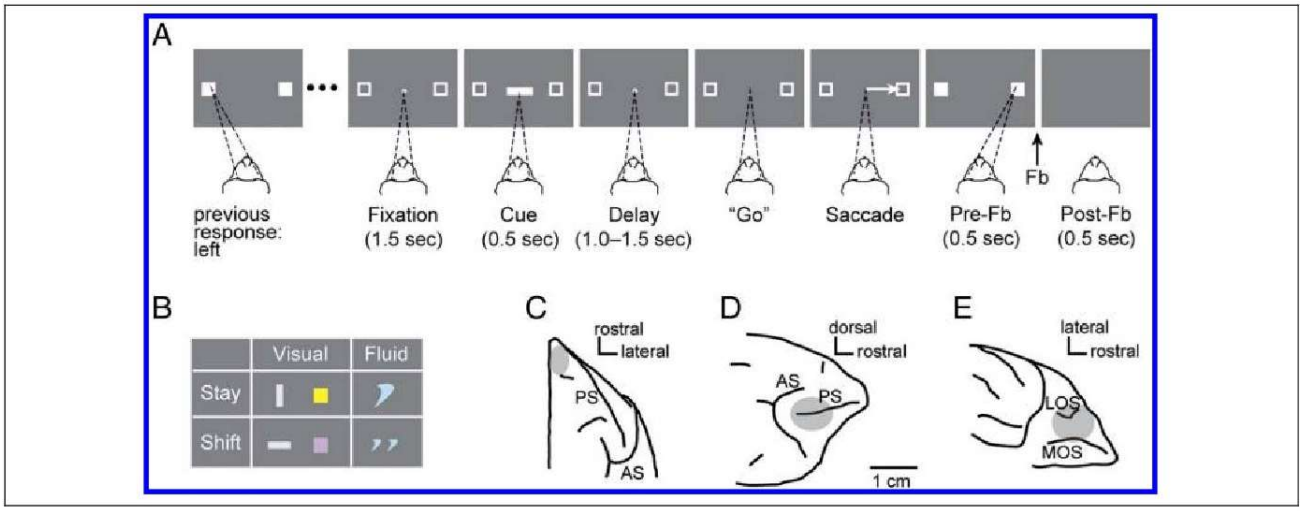

Figure 1. Behavioral task, cues used, and recording locations. (A) Example sequence of task events for the visually cued strategy task, from left to right. Each dark gray rectangle represents the video monitor as viewed by the monkey. Dashed lines indicate the target of the monkey's gaze. (B) Cues used in the task. In the visually cued strategy task, colored shapes instructed which strategy should be applied. In the fluid-reward cued strategy task, two half-drops of fluid instructed the shift strategy and a single drop instructed the stay strategy. (C–E) Recording zones for PFp (C), PFdl (D), and PFo (E). Fb = feedback; LOS = lateral orbital sulcus; MOS = medial orbital sulcus; PS = principal sulcus.

blocks of the fluid-reward cued task, stay and shift cues were intermixed pseudorandomly, and both occurred on approximately half of the trials. Hence, the left and right responses also occurred with a similar probability.

In both tasks, the monkeys were required to maintain fixation on the central spot for the entire cue period (0.5 sec), as well as for a subsequent delay period of 1.0, 1.25, or 1.5 sec, selected pseudorandomly. The fixation window was a ±3° square area centered on the fixation point; however, in practice both monkeys maintained fixation much more accurately than that requirement and only rarely made a saccade within the fixation window (Tsujimoto et al., 2009). Fixation breaks during the cue or delay periods aborted the trial.

The fixation spot and the two potential saccade targets remained on the screen during the delay period. The disappearance of the fixation spot served as the go signal, which triggered a saccadic eye movement to a target. Once the monkey made a saccade into a window (±3.75°) centered on one of the two potential targets, both targets became solid white whether the monkey correctly or incorrectly selected the goal on that trial. Entry of gaze into the response window was designated as target acquisition, and the monkey had to maintain target fixation for 0.5 sec. Fixation breaks during this pre-feedback period of 0.5 sec aborted the trial. Once target fixation exceeded 0.5 sec, a single drop of fluid (0.2 mL) was delivered as reward feedback after correct responses. After errors, the presentation of red squares over both targets provided negative feedback. On some blocks of the fluid-reward cued task, reward feedback was, like the cues for that task, either a single drop of fluid (0.2 mL) or two half-drops (0.1 mL each), selected pseudorandomly. Because the number of drops was pseudorandomly determined for both cue and feedback, all combinations of drop number occurred with roughly equal frequency.

After errors, the cue from that trial was repeated on a correction trial, which was presented until the monkey obtained a reward by responding correctly. In practice, the monkeys rarely required more than one correction trial after an error (Tsujimoto et al., 2009). The correction trials were excluded from all the analyses in this report.

The visually cued and fluid-reward cued tasks were presented to the monkeys in separate blocks of trials. Blocks in the visually cued strategy task consisted of a mean of 94 ± 19 (*SD*) trials; blocks in the fluid-reward cued strategy task averaged 55 ± 12 trials.

Data Collection

After the training was completed, we implanted a recording chamber (10.65 mm inner diameter) over the exposed dura mater of the PFp in the right hemisphere and recorded activity from this chamber. The detailed procedures for PFp, including chamber design, as well as the surgical and recording techniques, have been described elsewhere (Mitz et al., 2009). After the recording from PFp was completed, we implanted another chamber (18 mm inner diameter) over a more caudal part of the frontal lobe in the same hemisphere. The position and angle of this chamber were adjusted based on magnetic resonance images, so that both PFdl and PFo were accessible simultaneously through the same chamber (Tsujimoto et al., 2009).

Single-cell activity was recorded from up to 16 platinum–iridium electrodes (0.5–1.5 MΩ at 1 KHz; Thomas Recording, Giessen, Germany) simultaneously. The electrodes were individually inserted with a multielectrode drive (Thomas Recording) that enabled independent control of each electrode. In typical recording sessions for the caudal chamber, about half of the electrodes were advanced into PFo, whereas the others were maintained more superficially in PFdl.

Signals from each electrode were recorded using a Multichannel Acquisition Processor (Plexon, Dallas, TX). Single-cell potentials were isolated online and further sorted offline using a cluster cutting technique (Off Line Sorter, Plexon) based on multiple criteria, including PCA, the minimal interspike intervals, and close visual inspection of the entire waveforms for each cell.

Histology

The recording sites were reconstructed by histological analysis, which was supplemented by structural MRI. After data collection was completed, electrolytic lesions (20 μA for 20 sec, anodal current) were placed in selected locations at two depths per penetration in the caudal chamber. After 10 days, the monkey was deeply anesthetized and then perfused through the heart with 10% (v/v) formol saline. Immediately before and during the perfusion, a pin was inserted through the center of both the rostral and caudal chambers. The penetration sites and tracks were reconstructed in Nissl-strained sections by reference to recovered electrolytic lesions and to the marking pins inserted at the time of the perfusion. Cytoarchitectonic analysis confirmed that recording sites in PFo came from granular areas. The locations of recording sites have been described elsewhere (Tsujimoto et al., 2010, 2011a).

Data Analysis

Correction trials and error trials were excluded from all analyses reported here, which were performed using MatLab (The MathWorks, Inc., Natick, MA).

In this study, we mainly focused on the cells that showed goal-selective activity during the feedback time. The selection criteria for these cells were described previously (Tsujimoto et al., 2009, 2010, 2011a, 2012). Briefly, several task periods were first defined on the basis of time windows relative to task events; that is, a fixation period (0.5–1.0 sec after fixation onset), a cue period (0.0–0.5 sec after cue onset), a delay period (0.0–1.0 sec after

cue offset), and a feedback period (from 0.3 sec before feedback onset until 0.2 sec afterward). Then we compared mean activity rates between those four task periods using the Kruskal–Wallis test ($\alpha = 0.05$), which identified task-related neurons. Second, for all task-related neurons, we performed a two-factor ANOVA ($\alpha = 0.05$) for the feedback period activity. The factors were Goal (left or right) and Strategy (stay or shift). The cells that showed a main effect of Goal during the feedback period were classed as goal-selective.

As a measure of goal selectivity for those neurons, we computed the area under the receiver operating characteristic (AUROC) curve. ROC values measure the ability to detect a signal based on single-trial activity, independent of a cell's mean discharge rate or its dynamic range. Ideally, an ROC value of 0.5 would indicate no selectivity and a value of 1.0 would reflect absolute selectivity. However, because the ROC curves were computed based on preferred and antipreferred responses, a positive bias was introduced. This bias could have been corrected by a shuffling procedure, but the current analysis was not affected by such correction and the result here is based on the data without correction. Nevertheless, we have confirmed that the result did not change even if we adopted the correction with shuffled (10,000 times) data.

The trial-to-trial variability of the firing rate, as measured by spike counts, was evaluated by the Fano factor (FF). FF is defined as the spike count variance across trials divided by the mean within each time bin. In this study, the spike counts were computed in a 200-msec sliding window moving in 20 msec steps. We chose this relatively large window based on both a previous study for PFC cells (Hussar & Pasternak, 2010) and on our preliminary assessment using different window durations. As the spike counts in PFC are relatively low, the use of this window minimized artifacts and improved statistical power, although we confirmed that the key findings of this report were preserved using narrower time windows. The windows that contained no spikes (approximately 3% of the total sample) were excluded from the analysis.

To compare FF between tasks at different times across a trial, we selected eight time windows (i.e., 200-msec bins) for parts of the analysis. Each of these eight windows centered on (1) 400 msec before cue onset, (2) 100 msec after cue onset, (3) 100 msec after delay onset, (4) 600 msec after delay onset, (5) 400 msec before target acquisition, (6) 400 msec before feedback, (7) 100 msec after feedback, and (8) 600 msec after feedback. For the comparisons in multiple time windows, the alpha level was corrected by the Bonferroni method.

RESULTS

Behavior

Details of the behavioral results have been described previously (Tsujimoto et al., 2009, 2012). Briefly, both monkeys performed the visually cued strategy task proficiently, averaging greater than 90% correct responses. In the fluid-reward cued strategy task, the performance of the first monkey nearly matched this level. The second monkey made more errors on this task but still performed significantly above chance level. Oculomotor RTs were similar for the two strategies and for early and late recordings sessions. Both monkeys maintained stable and accurate fixation throughout the fixation and cue periods, within $\pm 1^\circ$ on more than 90% of the trials.

Neuronal Database

Our database consisted of 957 (569 and 388 from Monkeys 1 and 2, respectively) and 491 (345 and 146 from Monkeys 1 and 2, respectively) neurons that were related to visually cued and fluid-reward cued tasks, respectively. Of these, for the visually cued task, 274 cells were located in PFp, 405 in PFdl, and 278 in PFo. For the fluid-reward cued strategy task, 143 were recorded from PFp, 186 from PFdl, and 162 from PFo. Among this sample, approximately 30% of the cells showed goal-selective activity during the feedback period.

Properties of FF in PFp Cells with Goal-selective Feedback Period Activity

Figure 2A provides an example of a PFp neuron that showed goal-selective activity during the feedback period. Its mean firing rate, recorded during the visually cued task, was significantly higher during the feedback period for the left goal than for the right goal (two-way ANOVA, $p < .001$). However, FF was nearly at the baseline for both right and left goals during the feedback period, and there was no significant difference between left and right goals. Thus, as reported previously (Chang, Armstrong, & Moore, 2012; Churchland et al., 2010), FF behaved differently than the mean firing rate.

The cell in Figure 2B, recorded during the fluid-reward cued task, showed similar tendency. Although the mean firing rate during the feedback period was significantly different between left and right goals (two-way ANOVA, $p < .001$), FF was not significantly different.

To examine whether such a trend is present among the population of sampled neurons, we then plotted the population-level profile for the PFp cells that had goal selectivity during the feedback period (Figure 3). The goal choice that was associated with higher and lower firing rates was designated as preferred and antipreferred, respectively, and the population means for both firing rate (Figure 3A) and FF (Figure 3B) were computed separately for preferred and antipreferred goals, based on firing rate. The tendency observed in the single-cell examples (Figure 2) was replicated at the population level. Whereas the firing rate was clearly different between preferred and antipreferred responses during the feedback

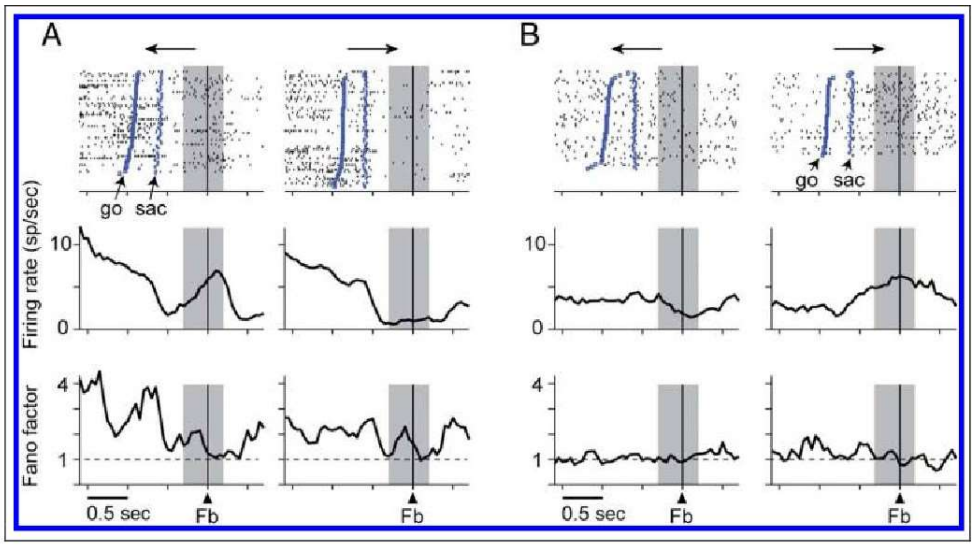

Figure 2. Firing rate and variability (FF) of two PFp neurons, each shown separately for goal (left or right, indicated by arrow at the top). In each panel, time is aligned on the reward feedback (Fb) indicated by marks on each raster line. Top panels show raster displays of spike times with trials sorted according to the saccadic RT. Timing of the go signal (go) and saccade onset (sac) is shown by the square over each raster line. Below raster plots, firing rate and variability are shown in the same format. Gray backgrounds indicate feedback period. Dashed line in FF indicates a baseline of 1.0. (A) A PFp neuron recorded during the visually cued strategy task. This neuron's firing rate showed a preference for the left goal chosen during the feedback period, regardless of strategy. (B) A PFp neuron recorded during the fluid-reward cued strategy task. The firing rate of this neuron preferred the right goal chosen during the feedback period.

time (a necessary consequence of selecting goal-selective PFp cells for this analysis; Figure 3A), FF showed a similar level for the two goals (Figure 3B). Viewed across task periods, FF showed a slight decrease during the feedback period regardless of the cell's firing rate encoding of the chosen goal, although this decrease did not go beyond the bracket of 95% confidence in any other task periods.

The firing rate of the PFp cells was not different between stay and shift trials, and our analysis also did not reveal any significant difference (i.e., not beyond the bracket of 95% confidence interval) in FF or between stay and shift trials. This was the case in both cue and delay periods and in visually cued and fluid-reward cued tasks.

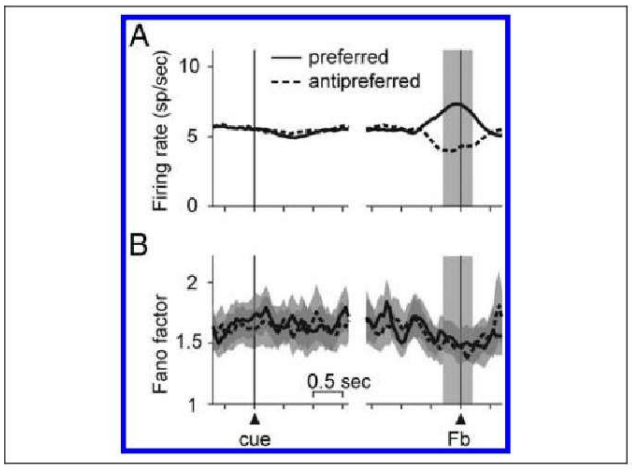

Figure 3. Population histograms for PFp cells that had goal-selective activity during the feedback period, firing rate (A) and FF (B). Each measure is shown separately for preferred and antipreferred chosen goals of each cell's firing rate during the feedback period. Each panel is aligned by cue and feedback (Fb) time. Shading behind the curve denotes the upper and lower limit of the 95% confidence interval, and the gray background denotes the feedback period.

Because FF did not differ significantly for the two goals (nor for strategies), data for subsequent analyses were collapsed across goals.

The temporal profile at the population level (Figure 3) could result from at least two different scenarios. On the one hand, each cell in this population could generally have a similar trend across trials. On the other hand, different subsets of cells could contribute differently to each task period, where, for example, one group decreased FF specifically during the feedback period whereas others did so during the cue period. To examine this point, we tested whether the FF level was similar across task periods on a cell-by-cell basis. Figure 4 plots FF for each cell during the cue (left panels) and feedback (right panels) periods against the corresponding FF during the pre-cue fixation period. FF during both the cue and feedback periods was significantly correlated with that in the pre-cue fixation period in both the visually cued (Figure 4A) and fluid-reward cued (Figure 4B) tasks. Thus, in PFp, the general cell-by-cell trend in FF was maintained across task periods from the fixation period until feedback time.

Comparison with Cells Lacking Goal Selectivity

Thus far, the results showed that FF values of goal-selective PFp cells have a general trend that behaves differently than the mean firing rate. If this FF trend is different from the other population of cells, it may provide some insight into the role of the goal-selective PFp population and eventually into the role of PFp overall.

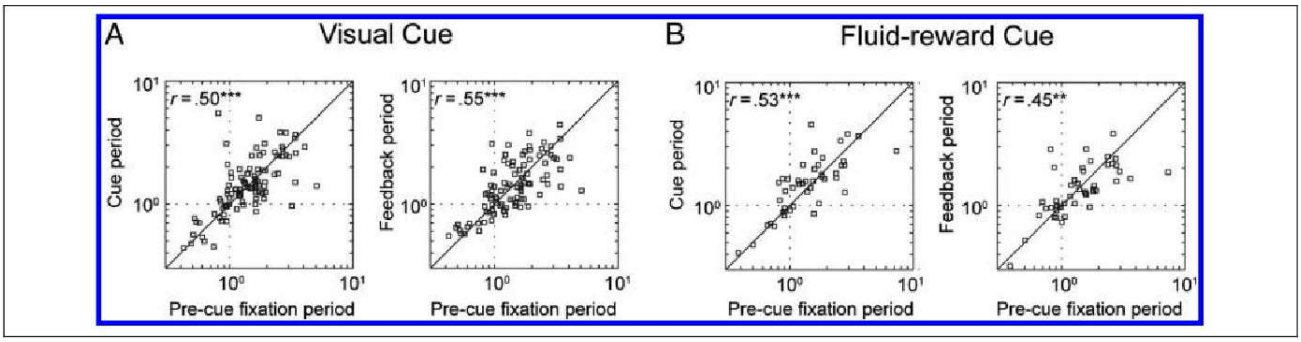

Figure 4. Cell-by-cell intratrial correlation of FF across task periods for PFp cells with goal-selective feedback period activity. The plots denote each neuron's FF value for cue (left) and feedback (right) period against the pre-cue fixation period, plotted on a log–log scale, with the Pearson's correlation coefficient (r) noted in each panel. (A) Visually cued task (n = 100). (B) Fluid-reward cued task (n = 47). ***p < .001, **p < .01.

To this end, we next compare FF of goal-selective PFp cells with that of the remaining PFp cells in our sample.

Panels A and B of Figure 5 plot FF values for those two populations separately. For the visually cued task, FF for the goal-selective population was continuously below the remaining population (Figure 5A). However, the data from the fluid-reward cued strategy task did not show this difference (Figure 5B).

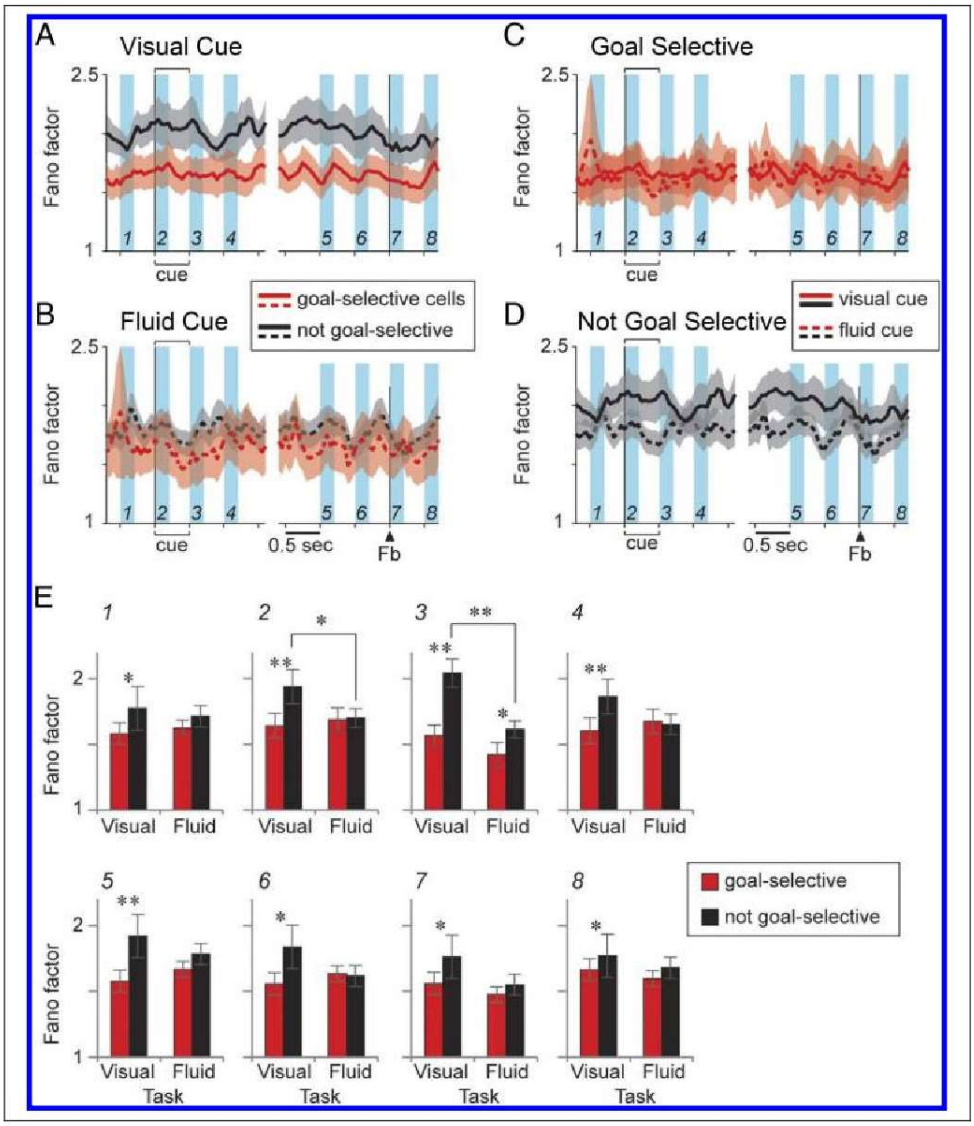

Figure 5. Comparison of FF between cells with goal selectivity and the remaining population of cells. (A) Population averages for PFp cells recorded during the visually cued strategy task (n = 100 for goal-selective and n = 147 for non-goal-selective populations). Each panel is aligned by cue and feedback (Fb). The factor of goal choice (left vs. right) was collapsed in this chart. Shading behind the curve denotes the range of the 95% confidence interval. Blue background indicates the time windows used for the analysis shown in E. Brackets above and below the plot mark the time that the visual cue was on. (B) The same plot as in A, but for cells recorded during the fluid-reward cued task (n = 47 for goal-selective and n = 96 for non-goal-selective populations). (C) The same plot as in A and B, but for goal-selective cells, shown separately for each task. (D) The same plot as in C, but for non-goal-selective cells. (E) Bar chart for FF at each of the eight time windows indicated by the blue background in A–D. **p < .01, *p < .05 (Bonferroni corrected).

Panels C and D of Figure 5 replot the same data sorted by the two populations of neurons; that is, goal selective and non-goal selective. The task-to-task difference shown in Figure 5A and B mainly resulted from the FF for cells without goal selectivity; the non-goal-selective population tended to show higher FF in the visually cued task than in the fluid-reward cued task (Figure 5D), whereas the FF level and trend for goal-selective cells were nearly identical in the two tasks (Figure 5C).

Figure 5E presents statistical tests of this tendency for eight time windows (200 msec each; see Methods) across the trial, as indicated by the blue shading in Figure 5A. For all windows in the visually cued task, FF was significantly lower in goal-selective cells than in the cells without goal selectivity (Mann–Whitney U test, $p < .05$, Bonferroni corrected). In contrast, for the fluid-reward cued task, this difference only reached significance immediately after cue offset (Window 3 in Figure 5E). A task versus task reduction in FF for cells lacking goal selectivity was statistically significant during and just after the cue period (Windows 2 and 3 in Figure 5E, black bars).

Although FF showed a significant difference between two groups of neurons throughout the trial in the visually cued task (Figure 5A, E), it could result from the difference in firing rate. To test this possibility, we compared the mean firing rates of those populations of cells during the fixation period. The firing rate for the goal-selective PFp cells was not significantly different from that for the remaining PFp cells in our sample (5.17 ± 6.93 (*SD*) spikes/sec vs. 4.49 ± 5.56 spikes/sec, for goal-selective vs. non-goal-selective cells, respectively; $t(546) = 1.26$, $p = .21$). Likewise, none of the other task periods showed a significant difference in firing rate between the two populations.

Comparison with PFo and PFdl

In previous work (Tsujimoto et al., 2009, 2012), we observed goal-selective firing activity during the feedback period in PFdl and PFo as well as PFp. Their activity was similar to that of the goal-selective PFp population—the focus of attention here—at least in the correctly responded trials, although there were some differences in error trial activity between areas. However, it is possible that FF may show different properties across these areas. Hence, we sought to examine the FF properties of goal-selective cells in PFdl and PFo and compare them with PFp cells.

Figure 6 shows the population data for the firing rate and FF for PFdl (Figure 6A) and PFo (Figure 6B) cells that showed goal selectivity during the feedback time. The profiles for both firing rate and FF were quite similar for PFdl and PFo. By selection of the cells, there was a clear difference in mean firing rate between preferred and antipreferred responses around the feedback time, showing a marked increase for preferred goals and a slight decrease for antipreferred goals. In contrast, FF showed a decrease around the feedback time regardless of the preference encoded by firing rate, as observed in PFp.

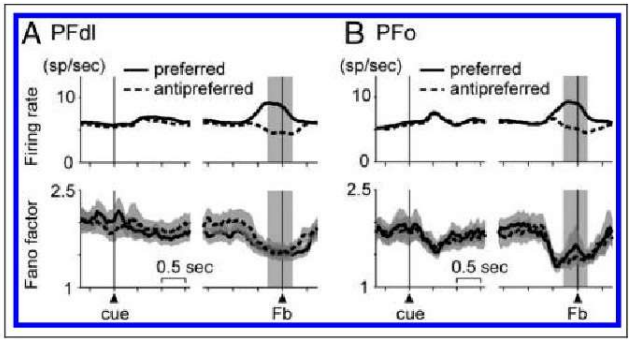

Figure 6. Population plot for firing rate and FF for PFC cells with goal-selective feedback period activity. Format as in Figure 3. (A) PFdl cells ($n = 144$). (B) PFo cells ($n = 79$).

Figure 7 shows the cell-by-cell consistency of FF across task periods for PFdl (Figure 7A) and PFo (Figure 7B), corresponding to the findings for PFp illustrated in Figure 4. PFdl cells yielded similar results to PFp, showing significant correlation across task periods in both the visually cued and the fluid-reward cued tasks (Figure 7A). In contrast, in PFo, FF during the fixation period significantly correlated only with the cue period, but not with the feedback period, suggesting that FF for those PFo cells during the feedback time was independent of FF during the fixation period.

We then tested whether FF for those PFo and PFdl cells differed from the cells without goal selectivity during the feedback period, as observed in the PFp population (Figure 5). However, in contrast to PFp, neither PFdl (Figure 8A) nor PFo (Figure 8D) showed this property in the visually cued task. Rather, in PFdl, the goal-selective cells had an even higher FF value than the cells without goal selectivity later in the task (Windows 5–7 in Figure 8C).

In the fluid-reward cued task, PFdl cells with goal-selective feedback period activity showed a decrease in FF after a reward was delivered as a cue (Window 3 in Figure 8B, C). This decrease was not observed when a reward was delivered as feedback. Instead, those cells showed an even higher FF level before feedback delivery than did other cells (Window 6 in Figure 8B, C). In contrast, PFo cells with such activity showed an apparent decrease in FF for both reward as cue and reward as feedback (Figure 8E, F), although the difference did not reach significance because of high cell-to-cell variability.

Correlation between Firing Rate Selectivity and FF

Thus far, the results indicate that in PFp—but not in either PFdl or PFo—FF for the cells with goal-selective feedback period activity differed from FF for the cells that lack goal

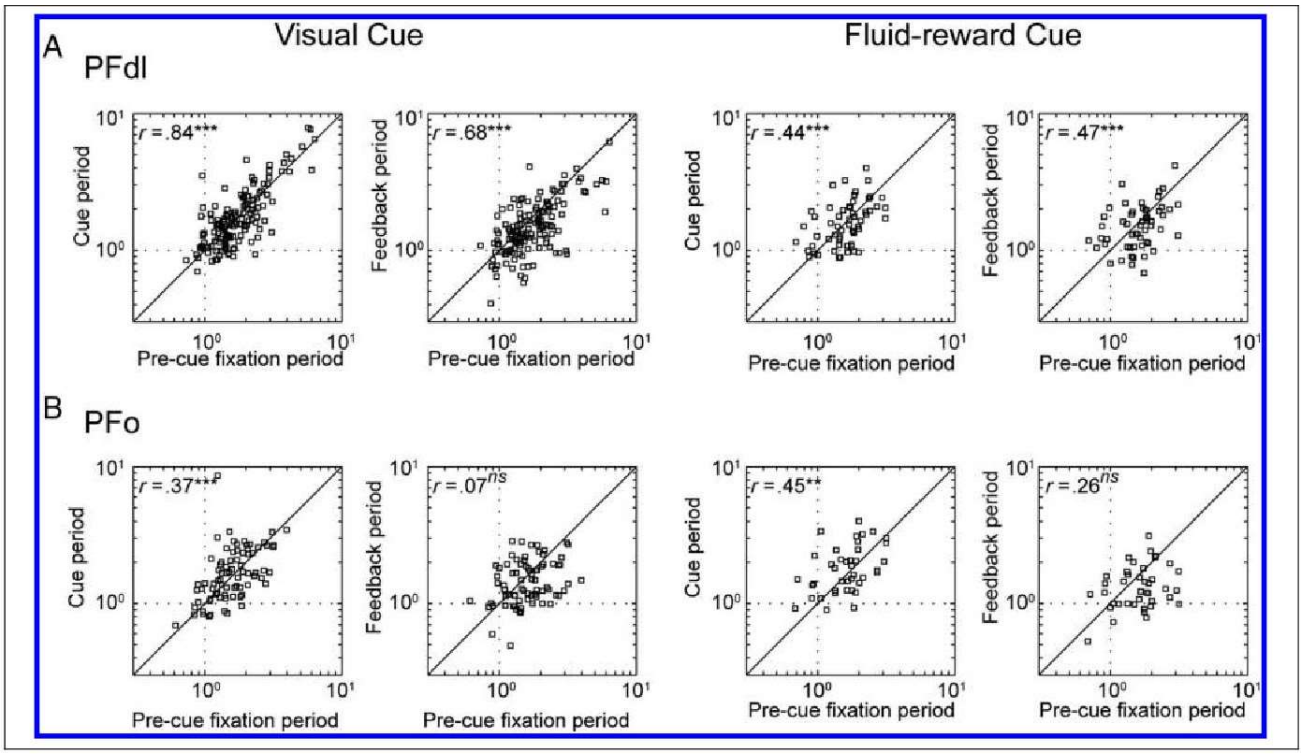

Figure 7. Cell-by-cell intratrial correlation of FF across task periods for PFC cells with goal-selective feedback period activity. Format as in Figure 4. (A) PFdl cells (n = 144). (B) PFo cells (n = 79).

selectivity, at least as judged by firing rate modulations (Figure 5A). We then examined whether the strength of the goal selectivity in terms of firing rate was correlated with FF using the AUROC as an index for the goal selectivity, as judged by firing rate.

Figure 9 plots the correlation coefficient of the AUROC with FF during the last 200-msec bin of the minimal delay period (i.e., 800–1000 msec after delay onset, which also corresponded to cue offset). This window was chosen because it is the latest 200 msec period before the go cue might occur, which it did at that time on approximately one third of the trials. In the visually cued task (Figure 9A), the Pearson's correlation coefficient (r) was $-.26$ ($p = .009$). This inverse correlation, although relatively weak, was still significant even after the outlier was taken into consideration by the percentage bend method (Pernet, Wilcox, & Rousselet, 2012; $r = -.20$, $p < .05$).

The same tendency was observed in the fluid-reward cued task (Figure 9B). The entire data set did not reach statistical significance in Pearson's correlation ($r = -.27$, $p = .07$). To explore whether a few points with unusually high variance to mean ratios influenced this marginally nonsignificant result, we again applied the percentage bend technique (Pernet et al., 2012). This analysis showed a statistically significant correlation ($r = -.32$, $p < .05$), which points to an underlying trend in the data, if not a statistically significant one. Note that, regardless of significance testing, the correlation depicted in Figure 9A was weak, accounting for less than 7% of the variance in the bivariate data.

In contrast, these variables showed no relationship at all in PFdl (Figure 9C, D) and PFo (Figure 9E, F) for either task (for all cases, $-.1 < r < .1$, $p > .1$; see the figure legend for exact r and p values).

DISCUSSION

We examined a measure of firing rate variability, FF, in three PFC areas as monkeys performed a cued-strategy task. When compared with the remaining population of cells in PFp, goal-selective PFp cells showed lower variability during the visually cued task. Unlike their firing rate modulation, this difference in FF was observed not only during the peri-feedback period, but also from the beginning of the trial (Figure 5). In contrast, neither PFdl nor PFo showed any systematic difference in FF between goal-selective cells and the remaining population (Figure 8). Furthermore, in PFp—but not in PFdl or PFo—a stronger degree of goal selectivity during feedback time was associated with a lower FF earlier in the trial (i.e., at the end of the delay period; Figure 9). These findings suggest that the goal-encoding population of PFp neurons is engaged in the task throughout each trial, a property that could both increase the fidelity of goal encoding and the ability to link a goal choice with the context and strategy used to choose that goal.

The decrease in FF during the peri-feedback period, which occurred in all three areas, resembles results from previous studies. For example, Steinmetz and Moore (2010) reported FF reduction in V4 before saccades regardless of their direction, although the mean firing rate differed by direction. Likewise, Hussar and Pasternak (2010) reported that PFdl neurons encoding the motion of visual stimuli showed reduced FF during the stimulus presentation, regardless of whether motion was in the cell's preferred direction.

Taken together with the relatively low firing rates in PFC neurons, especially those in PFp (Tsujimoto et al., 2010), the FF modulation observed here is unlikely to be directly affected by mean firing rate. The finding that a stable decrease in FF was not accompanied by a change in firing rate has been reported previously. There was overall reduction of FF in PFC cells during a working memory task, for example, when pre- and posttraining data were contrasted (Qi & Constantinidis, 2012). Hussar and Pasternak (2010) also reported that an anticipatory decline in FF, without rate modulation, preceded a stimulus-induced decline. Among the three PFC areas examined here, only PFp showed this overall trend; we return to this topic below.

However, during the fluid-reward cued task, we did not observe an overall difference in FF in the PFp cells with versus without goal selectivity (Figure 5). This task-to-task difference mainly resulted from the FF for cells without goal selectivity. We describe this result as a decrease in FF in the goal-selective cells because FF levels in all the tested populations in PFdl and PFo were comparable to those in PFp cells without goal selectivity during the visually cued task. Following discussion of this goal-selective population, we also discuss FF reduction of cells without goal selectivity in the fluid-reward cued task.

Although we found that PFdl and PFo contain different populations of neurons, which encode, for example, the strategy cued and/or the upcoming responses (Tsujimoto

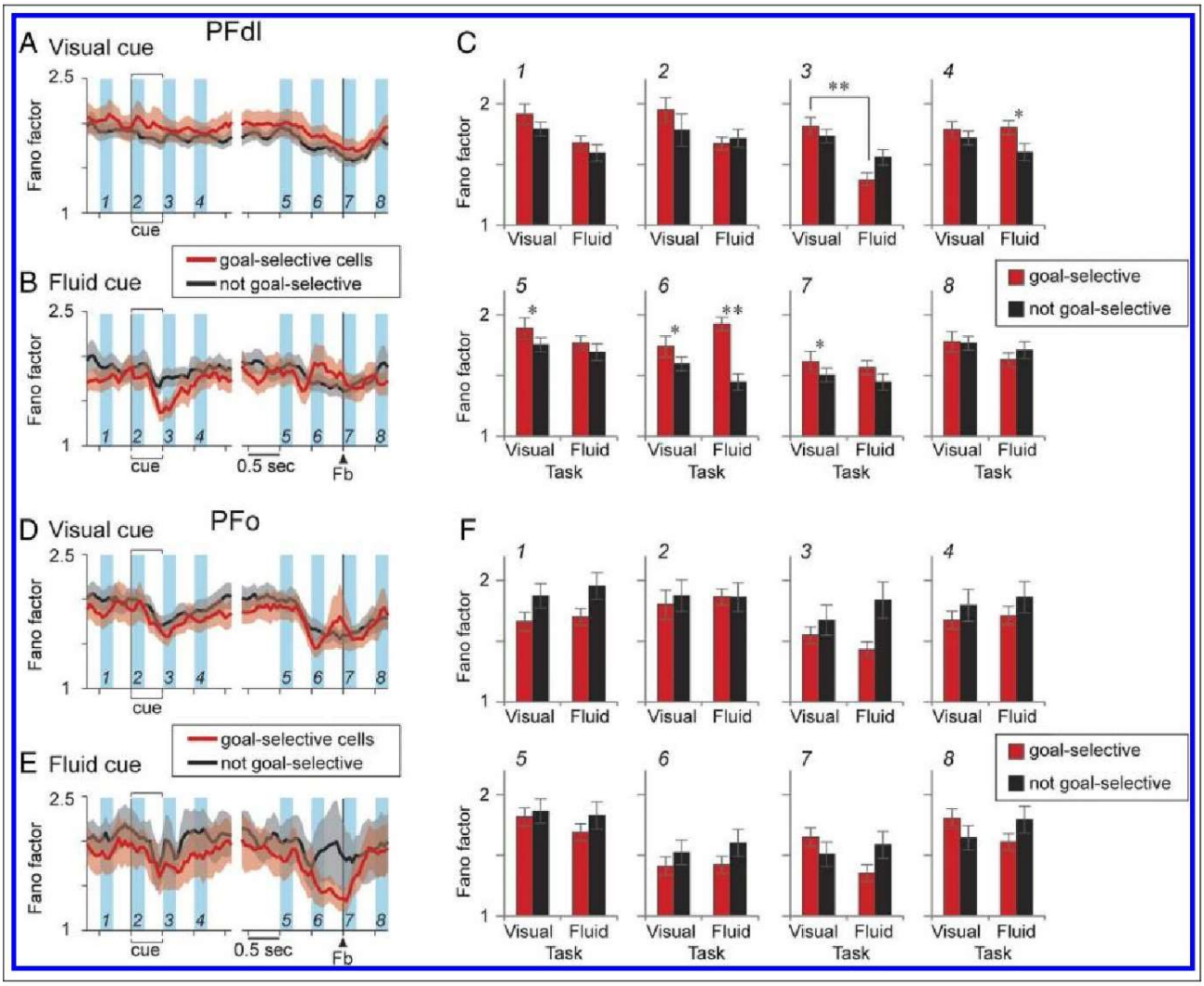

Figure 8. (A–F) Comparison of FF between cells with goal selectivity and the remaining population of cells for PFdl (A–C) and PFo (D–F). Format as in Figure 5. $^{**}p < .01$, $^{*}p < .05$ (Bonferroni corrected).

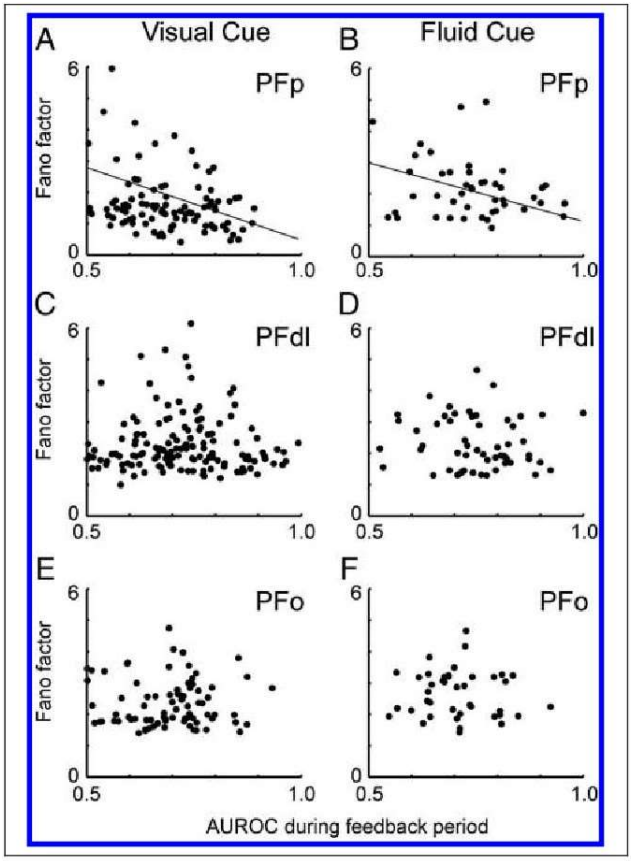

Figure 9. Scatter plots for FF during the delay period against AUROC during the feedback period. The last bin of the minimal delay period was used for this analysis. (A) PFp cells in the visually cued task. (B) PFp cells in the fluid-reward cued task. (C) PFdl cells in the visually cued task ($r = -.03$, $p = .71$). (D) PFp cells in the fluid-reward cued task ($r = -.08$, $p = .53$). (E) PFo cells in the visually cued task ($r = -.01$, $p = .94$). (F) PFo cells in the fluid-reward cued task ($r = -.06$, $p = .70$).

et al., 2011a, 2012), we do not focus on these cells in this report.

Implications for PFp Function

In our previous study, the mean firing rate of PFp cells did not encode task-related information until after the monkey's saccade (Tsujimoto et al., 2010). On the other hand, FF showed a lower level well before goal selection in the population of PFp cells that later in the trial encoded the chosen goal, but not in PFdl and PFo cells with similar activity. In the premotor cortex and the FEF, trial-to-trial variability is known to be a signature of motor preparation. In these areas, FF reaches a minimum immediately before the movements (Purcell et al., 2012; Churchland et al., 2006). In addition, FF in such areas predicts the monkey's RT better than mean firing rate (Marcos et al., 2013; Purcell et al., 2012; Steinmetz & Moore, 2010; Churchland et al., 2006). By analogy, FF reduction in PFp cells during the premovement phase of the trial may reflect the preparation for an upcoming event that is important for the function of this particular brain area. A candidate for this event is a goal choice, as our task required the monkey to monitor the goal that it had chosen on the previous trial and hold it in memory until the next trial.

Consistent with this view, the strength of goal selectivity, as assessed by firing rate during the feedback period, was significantly and inversely correlated with FF earlier in the trial (Figure 9A, B). A previous study of PFC cells suggested that trial-to-trial variability reflects engagement of the neurons in the components of the ongoing task (Hussar & Pasternak, 2010). FF reduction in PFp cells during the early phase of a trial may reflect the preparatory state of those cells for upcoming goal choice, linked to the process that guides that choice.

PFdl and PFo cells differed from PFp cells in several ways. Notwithstanding the fact that PFdl and PFo also contain a population of cells that encode chosen goals during the feedback period, the strength of the goal selectivity did not correlate with FF earlier in a trial. Furthermore, PFo cells did not show intratrial correlation of FF values between the feedback period and earlier task periods (Figure 7B). Therefore, among three areas, only the overall FF reduction in PFp neurons across the trial suggested an increased engagement of those neurons in the task, which could in turn contribute to goal encoding.

This across-area difference in FF of the feedback-related goal-selective cells appears to be consistent with the across-area difference in firing patterns in the same population of cells. In our previous reports (Tsujimoto et al., 2011a, 2012), detailed analyses on the goal-selective feedback period firing activity indicated that PFp—but not PFdl or PFo—encoded the feedback (reward or error signal) before feedback arrives. Such prefeedback coding must reflect some internal signal about the monkey's own response because no external event provided such information until feedback delivery. In fact, human neuroimaging studies have suggested the role of PFp, especially its medial parts, in stimulus-independent, internal thought processes (Mason et al., 2007; Gilbert et al., 2006; Christoff, Ream, & Gabrieli, 2004). The FF reduction of the goal-selective PFp cells is likely to be related to such internal thought processes.

Thus, the present finding of FF reduction in the PFp population from the earlier phase of the task concurs with the findings from monkey neurophysiology as well as human neuroimaging and may provide further support for the previously proposed model (Tsujimoto et al., 2012), where the goal-selective activity of PFp cells could promote learning about which kind of response-generating cognitive processes produced a given outcome (Tsujimoto et al., 2011b). In this proposed model, such a synthetic goal signal in PFp is assumed to be used by the posterior PFC parts, such as PFdl and PFo, to guide the correct response in the forthcoming trial, because the firing rate of their cells encodes cued strategy and future responses (Tsujimoto et al., 2012). The lower FF in PFp population

could improve the ability of other cortical areas to decode its selected-goal signal.

In contrast to the PFp population, PFo cells with goal-selective feedback period activity appeared to subserve the assignment of response choices to outcome (Wallis, 2012; Walton, Behrens, Buckley, Rudebeck, & Rushworth, 2010), and PFdl cells with such activity encoded the response–outcome conjunction, which is the information necessary for the next trial in our task. These roles of PFdl and PFo cells concur with the present finding that FF reduction was not observed in these areas in the earlier task periods.

In the fluid-reward cued task, in addition to the goal-selective population in PFp, the remaining cell population, which did not have goal-selective rate modulation during the feedback period, also showed a decreased FF value in the earlier parts of a trial (Figure 5B). Reward delivery is a critical event to the monkey, and so it seems likely that the PFp cells without goal-selective firing activity are involved in preparation for receiving a reward during the cue period. It is notable that, when we compare the FF of non-goal-encoding cells, a significant difference was observed between visual and fluid tasks at the beginning and immediately after the cue period (Figure 5E, panels 2 and 3). Previous studies have shown that multiple parts of the PFC contain cells that reflect the parameters associated with motivational context such as the current or future reward type (Watanabe, Hikosaka, Sakagami, & Shirakawa, 2002), the schedule of reward (Shidara & Richmond, 2002), or the time until reward (Hikosaka & Watanabe, 2004). This kind of activity is often observed throughout a trial from the pre-cue period, which resembles the FF reduction observed in this study. Considering that monkey PFp is likely to correspond to medial PFp of humans (Neubert, Mars, Thomas, Sallet, & Rushworth, 2014), which has been implicated in affective or emotional roles (Bludau et al., 2014), the FF reduction of the non-goal-selective PFp cells in the fluid-reward cued task may participate in the processing of motivational context.

Two recent studies have reported the effects of PFp lesions on monkey behavior (Boschin, Piekema, & Buckley, 2015; Mansouri, Buckley, Mahboubi, & Tanaka, 2015). Mansouri et al. showed that PFp-lesioned monkeys can perform an analog of the WCST as well as intact controls. Moreover, PFp-lesioned monkeys showed even better performance than the control monkeys when they faced interruptions by a newly introduced secondary task or by unexpected reward delivery. Mansouri et al. interpreted these results as support for the idea that PFp may be involved in the redistribution of cognitive resources from the current task to other competing tasks. This interpretation agrees with the FF variability profile in PFp in the following sense. PFp cells showed reduction in variability from the beginning of a trial even before the cue, which implies that the cells are "ready" to process unexpected events. There was no interrupting event in our task, and hence, the cells might show modulation in firing rate only in response to the goal choices. To test this possibility, further recording studies will be needed with branching and related tasks.

On the other hand, Boschin et al. (2015) suggested that PFp mediates exploration and evaluation of the relative value of alternatives, particularly when the alternatives are novel (also see Boschin & Buckley, 2015). Because our task included neither exploration nor evaluation of alternatives, we are not able to examine our data from this point of view. Nevertheless, our hypothesis does not conflict with this idea because it postulates that the PFp cells are in a preparatory state for processing new events even before goal choice, which would allow them to flexibly participate if novel stimuli appear.

Conclusion

A measure of neuronal variability showed another feature that distinguished PFp neurons from those in PFdl and PFo. In PFp, unlike firing rate modulation, FF variability showed changes from the early period in a trial. This variability was correlated with an index of goal selectivity calculated from the firing rate later in the task, which implies that the variability reflects an important function of PFp. PFp, especially its medial part, in humans comprises a key part of the default mode network, and it shows a decrease in activation (as assessed by changes in blood flow or metabolism) when subjects are engaged in a task (Power, Schlaggar, & Petersen, 2014; Shulman et al., 1997). Our results contribute to this idea by suggesting that the neural circuit becomes less noisy during a task, even though the firing activity or a BOLD (blood flow) signal decreases. A less noisy state of this kind would provide an efficient link between goal choices and a preceding context that guides that choice. In a broader framework, lower FF variation might play a role in the flexible adaptation to novel events or intervening tasks (Boschin et al., 2015; Mansouri et al., 2015).

Acknowledgments

We thank Dr. Steven P. Wise for his support during all phases of this project, as well as Dr. Andrew R. Mitz, Mr. James Fellows, and Ms. Ping-Yu Chen for technical support. This work was supported in part by the Division of Intramural Research of the National Institute of Mental Health (Z01MH-01092) and in part by Grants-in-Aid from JSPS (15K12049 and 26282218) and ImPACT Program of Council for Science, Technology and Innovation (Cabinet Office, Government of Japan).

Reprint requests should be sent to Satoshi Tsujimoto, Department of Intelligence Science and Technology, Graduate School of Informatics, Kyoto University, Yoshida Honmachi, Sakyo-ku, Kyoto 606-8501, Japan, or via e-mail: s.tsujimoto@i.kyoto-u.ac.jp.

REFERENCES

Badre, D., & D'Esposito, M. (2009). Is the rostro-caudal axis of the frontal lobe hierarchical? *Nature Reviews Neuroscience, 10,* 659–669.

Bludau, S., Eickhoff, S. B., Mohlberg, H., Caspers, S., Laird, A. R., Fox, P. T., et al. (2014). Cytoarchitecture, probability maps and functions of the human frontal pole. *Neuroimage, 93,* 260–275.

Boschin, E. A., & Buckley, M. J. (2015). Differential contributions of dorsolateral and frontopolar cortices to working memory processes in the primate. *Frontiers in Systems Neuroscience, 9,* 114.

Boschin, E. A., Piekema, C., & Buckley, M. J. (2015). Essential functions of primate frontopolar cortex in cognition. *Proceedings of the National Academy of Sciences, U.S.A., 112,* E1020–E1027.

Chang, M. H., Armstrong, K. M., & Moore, T. (2012). Dissociation of response variability from firing rate effects in frontal eye field neurons during visual stimulation, working memory, and attention. *Journal of Neuroscience, 32,* 2204–2216.

Christoff, K., Ream, J. M., & Gabrieli, J. D. (2004). Neural basis of spontaneous thought processes. *Cortex, 40,* 623–630.

Christoff, K., Ream, J. M., Geddes, L. P., & Gabrieli, J. D. (2003). Evaluating self-generated information: Anterior prefrontal contributions to human cognition. *Behavioural Neuroscience, 117,* 1161–1168.

Churchland, M. M., Yu, B. M., Cunningham, J. P., Sugrue, L. P., Cohen, M. R., Corrado, G. S., et al. (2010). Stimulus onset quenches neural variability: A widespread cortical phenomenon. *Nature Neuroscience, 13,* 369–378.

Churchland, M. M., Yu, B. M., Ryu, S. I., Santhanam, G., & Shenoy, K. V. (2006). Neural variability in premotor cortex provides a signature of motor preparation. *Journal of Neuroscience, 26,* 3697–3712.

Desrochers, T. M., Chatham, C. H., & Badre, D. (2015). The necessity of rostrolateral prefrontal cortex for higher-level sequential behavior. *Neuron, 87,* 1357–1368.

Gilbert, S. J., Spengler, S., Simons, J. S., Steele, J. D., Lawrie, S. M., Frith, C. D., et al. (2006). Functional specialization within rostral prefrontal cortex (area 10): A meta-analysis. *Journal of Cognitive Neuroscience, 18,* 932–948.

Hikosaka, K., & Watanabe, M. (2004). Long- and short-range reward expectancy in the primate orbitofrontal cortex. *European Journal of Neuroscience, 19,* 1046–1054.

Hussar, C., & Pasternak, T. (2010). Trial-to-trial variability of the prefrontal neurons reveals the nature of their engagement in a motion discrimination task. *Proceedings of the National Academy of Sciences, U.S.A., 107,* 21842–21847.

Koechlin, E. (2016). Prefrontal executive function and adaptive behavior in complex environments. *Current Opinion in Neurobiology, 37,* 1–6.

Mansouri, F. A., Buckley, M. J., Mahboubi, M., & Tanaka, K. (2015). Behavioral consequences of selective damage to frontal pole and posterior cingulate cortices. *Proceedings of the National Academy of Sciences, U.S.A., 112,* E3940–E3949.

Marcos, E., Pani, P., Brunamonti, E., Deco, G., Ferraina, S., & Verschure, P. (2013). Neural variability in premotor cortex is modulated by trial history and predicts behavioral performance. *Neuron, 78,* 249–255.

Mason, M. F., Norton, M. I., Van Horn, J. D., Wegner, D. M., Grafton, S. T., & Macrae, C. N. (2007). Wandering minds: The default network and stimulus-independent thought. *Science, 315,* 393–395.

Mitchell, J. F., Sundberg, K. A., & Reynolds, J. H. (2007). Differential attention-dependent response modulation across cell classes in macaque visual area V4. *Neuron, 55,* 131–141.

Mitz, A. R., Tsujimoto, S., Maclarty, A. J., & Wise, S. P. (2009). A method for recording single-cell activity in the frontal-pole cortex of macaque monkeys. *Journal of Neuroscience Methods, 177,* 60–66.

Neubert, F. X., Mars, R. B., Thomas, A. G., Sallet, J., & Rushworth, M. F. (2014). Comparison of human ventral frontal cortex areas for cognitive control and language with areas in monkey frontal cortex. *Neuron, 81,* 700–713.

Pernet, C. R., Wilcox, R., & Rousselet, G. A. (2012). Robust correlation analyses: False positive and power validation using a new open source matlab toolbox. *Frontiers in Psychology, 3,* 606.

Power, J. D., Schlaggar, B. L., & Petersen, S. E. (2014). Studying brain organization via spontaneous fMRI signal. *Neuron, 84,* 681–696.

Preuss, T. M., & Goldman-Rakic, P. S. (1991). Myelo- and cytoarchitecture of the granular frontal cortex and surrounding regions in the strepsirhine primate Galago and the anthropoid primate Macaca. *Journal of Comparative Neurology, 310,* 429–474.

Purcell, B. A., Heitz, R. P., Cohen, J. Y., & Schall, J. D. (2012). Response variability of frontal eye field neurons modulates with sensory input and saccade preparation but not visual search salience. *Journal of Neurophysiology, 108,* 2737–2750.

Qi, X. L., & Constantinidis, C. (2012). Variability of prefrontal neuronal discharges before and after training in a working memory task. *PLoS One, 7,* e41053.

Qi, X. L., & Constantinidis, C. (2015). Lower neuronal variability in the monkey dorsolateral prefrontal than posterior parietal cortex. *Journal of Neurophysiology, 114,* 2194–2203.

Ramnani, N., Elliott, R., Athwal, B. S., & Passingham, R. E. (2004). Prediction error for free monetary reward in the human prefrontal cortex. *Neuroimage, 23,* 777–786.

Ramnani, N., & Owen, A. M. (2004). Anterior prefrontal cortex: Insights into function from anatomy and neuroimaging. *Nature Reviews Neuroscience, 5,* 184–194.

Shadlen, M. N., & Newsome, W. T. (1998). The variable discharge of cortical neurons: Implications for connectivity, computation, and information coding. *Journal of Neuroscience, 18,* 3870–3896.

Shidara, M., & Richmond, B. J. (2002). Anterior cingulate: Single neuronal signals related to degree of reward expectancy. *Science, 296,* 1709–1711.

Shulman, G. L., Fiez, J. A., Corbetta, M., Buckner, R. L., Miezin, F. M., Raichle, M. E., et al. (1997). Common blood flow changes across visual tasks: II. Decreases in cerebral cortex. *Journal of Cognitive Neuroscience, 9,* 648–663.

Steinmetz, N. A., & Moore, T. (2010). Changes in the response rate and response variability of area V4 neurons during the preparation of saccadic eye movements. *Journal of Neurophysiology, 103,* 1171–1178.

Tsujimoto, S., Genovesio, A., & Wise, S. P. (2009). Monkey orbitofrontal cortex encodes response choices near feedback time. *Journal of Neuroscience, 29,* 2569–2574.

Tsujimoto, S., Genovesio, A., & Wise, S. P. (2010). Evaluating self-generated decisions in frontal pole cortex of monkeys. *Nature Neuroscience, 13,* 120–126.

Tsujimoto, S., Genovesio, A., & Wise, S. P. (2011a). Comparison of strategy signals in the dorsolateral and orbital prefrontal cortex. *Journal of Neuroscience, 31,* 4583–4592.

Tsujimoto, S., Genovesio, A., & Wise, S. P. (2011b). Frontal pole cortex: Encoding ends at the end of the endbrain. *Trends in Cognitive Sciences, 15,* 169–176.

Tsujimoto, S., Genovesio, A., & Wise, S. P. (2012). Neuronal activity during a cued strategy task: Comparison of dorsolateral, orbital, and polar prefrontal cortex. *Journal of Neuroscience, 32,* 11017–11031.

Wallis, J. D. (2012). Cross-species studies of orbitofrontal cortex and value-based decision-making. *Nature Neuroscience, 15,* 13–19.

Walton, M. E., Behrens, T. E., Buckley, M. J., Rudebeck, P. H., & Rushworth, M. F. (2010). Separable learning systems in the macaque brain and the role of orbitofrontal cortex in contingent learning. *Neuron, 65,* 927–939.

Watanabe, M., Hikosaka, K., Sakagami, M., & Shirakawa, S. (2002). Coding and monitoring of motivational context in the primate prefrontal cortex. *Journal of Neuroscience, 22,* 2391–2400.

This article has been cited by:

1. Chihiro Hosoda, Satoshi Tsujimoto, Masaru Tatekawa, Manabu Honda, Rieko Osu, Takashi Hanakawa. 2020. Plastic frontal pole cortex structure related to individual persistence for goal achievement. *Communications Biology* **3**:1. . [Crossref]
2. Valentina Mione, Satoshi Tsujimoto, Aldo Genovesio. 2019. Neural Correlations Underlying Self-Generated Decision in the Frontal Pole Cortex during a Cued Strategy Task. *Neuroscience* **404**, 519-528. [Crossref]
3. Valeria Fascianelli, Satoshi Tsujimoto, Encarni Marcos, Aldo Genovesio. 2019. Autocorrelation Structure in the Macaque Dorsolateral, But not Orbital or Polar, Prefrontal Cortex Predicts Response-Coding Strength in a Visually Cued Strategy Task. *Cerebral Cortex* **29**:1, 230-241. [Crossref]
4. Rossella Cirillo, Valeria Fascianelli, Lorenzo Ferrucci, Aldo Genovesio. 2018. Neural Intrinsic Timescales in the Macaque Dorsal Premotor Cortex Predict the Strength of Spatial Response Coding. *iScience* **10**, 203-210. [Crossref]
5. Farshad Alizadeh Mansouri, Etienne Koechlin, Marcello G. P. Rosa, Mark J. Buckley. 2017. Managing competing goals — a key role for the frontopolar cortex. *Nature Reviews Neuroscience* **18**:11, 645-657. [Crossref]